Research article

LUMINESCENCE
The Journal of Biological and Chemical Luminescence

Received: 28 January 2016, Revised: 11 February 2016, Accepted: 21 February 2016 Published online in Wiley Online Library

(wileyonlinelibrary.com) DOI 10.1002/bio.3127

On–off Bodipy chemosensor for recognition of iron(III) ion based on the inner filter effect and its applications in cellular and bacterial imaging

Lingcan Kong,[a]* Keyu Lu,[b] Guangyuan Ma,[a] Yuyang Yao,[a] Xia Ling[a] and Wenwei Liu[a]*

ABSTRACT: One strong fluorescent Bodipy-containing derivative was synthesized and characterized using ^{1}H NMR, electrospray ionization mass spectrometry and elemental analysis. Its electrochemical and photophysical properties were investigated. In addition, the Bodipy derivative could be used as an on–off fluorescent probe for the detection of Fe^{3+} ions based on the inner filter effect because the absorption band of the Fe^{3+} ion overlaps the excitation band of Bodipy very well upon irradiation with UV light. Furthermore, the Bodipy-based sensor has obvious advantages including simplicity, rapid response, high selectivity, sensitivity and a detection limit of 1.2 μmol/L, and has been demonstrated in real water samples including tap water, mineral water and water from Lake Tai. Moreover, the fluorescent probe could also be used as a probe for the determination of Fe^{3+} in cellular and bacterial imaging. Copyright © 2016 John Wiley & Sons, Ltd.

Additional supporting information may be found in the online version of this article at the publisher's web site.

Keywords: Bodipy; fluorescent probe, iron(III); cellular imaging, bacterial imaging

Introduction

During past decades, many industrial and anthropogenic processes have released heavy metal ions into the environment (1–3). Iron is one of the most important of the transition metals because of its crucial roles in many biochemical processes including oxygen uptake, electron transfer and the catalysis of oxido-reductase reactions (4,5). Iron deficiency results in poor work performance and decreased immunity (6). However, excessive iron (III) ions are also hazardous to public health because of the association of iron with the development of severe diseases including various cancers, organ dysfunction and hepatitis (7–9). Therefore, the quantitative determination of iron(III) in environmental samples is of great importance and intense research efforts have been devoted to developing methods for iron(III) ion detection (10–12).

Compared with other techniques, fluorescent methods have a lot of advantages, such as high sensitivity and convenience (13). As a result, many fluorescent chemosensors have been employed for the detection of iron(III) ion by monitoring changes in their fluorescent intensity (14–16). Different photophysical processes, such as photoinduced electron transfer, intramolecular charge transfer, fluorescence resonance energy transfer and metal–ligand charge transfer, are constantly employed in fluorescent sensors (17–19). In general, the above sensing mechanism often involves the intermolecular interaction between the chemosensor and the target molecule. It works well only when there is proper geometry and distance. Thus, these methods are complicated and time-consuming, leading to restricted applications. An alternative way to design fluorescent chemosensors is based on the inner filter effect (IFE), which is known to result from the absorption of excited light and emission induced by the target molecule or ions in the detection system (20–22). This method often shows enhanced sensitivity relative to other methods because changes in the absorption of the sensors could transform into the exponential changes in the fluorescence intensity (23). In fact, the choice of chemosensor via fluorescent IFE is also crucial.

Relative to other organic dyes, Bodipys are an interesting class of materials possessing merits such as large molar absorption coefficients (ε), high quantum yields and other rich photophysical properties (24–26). These properties enable Bodipy-containing molecules to be used in the development of Bodipy-based fluorescent sensors by designing molecules accordingly (27). To make the synthesis easy, an IFE-based mechanism is employed. To the best of our knowledge, Bodipy-containing fluorescent sensors for Fe^{3+} ions based on IFE mechanism are very rare (28).

Recently, Bodipy derivatives have been successfully used in the fluorescent detection of metal ions based on the strong interaction between Bodipy derivatives and metal ions (29–31). By contrast, corresponding studies on the determination of metal ions using IFE, which has relative weak interaction between Bodipy derivatives and metal ions, were very rare. Furthermore, investigations

* Correspondence to: L. Kong and W. Liu, Wuxi Center for Disease Control and Prevention, Wuxi 214023, People's Republic of China. E-mail: konglingcan2010@163.com; liuwwcdc@126.com

[a] Wuxi Center for Disease Control and Prevention, Wuxi 214023, People's Republic of China

[b] State Key Laboratory of Food Science and Technology, Jiangnan University, Wuxi 214122, People's Republic of China

on cellular and bacterial imaging are also scarce. To the best of our knowledge, this work represents the first study on the detection of metal ions in cells and bacteria based on the IFE mechanism. Here, we present a novel Bodipy-containing fluorescent sensor **1** for Fe^{3+} ion determination in acetonitrile/water media (9:1 v/v) including real water such as tap water, mineral water and water from Lake Tai. This method is highly reproducible and the prepared compound **1** exhibits strong fluorescence in the absence of Fe^{3+}. Interestingly, the fluorescence is greatly quenched upon addition of Fe^{3+}. More importantly, the fluorescent sensor shows good sensitivity and selectivity in the presence of other metal ions, such as Mn^{2+}, Zn^{2+}, Pb^{2+}, Cr^{3+}, Er^{3+}, Yb^{3+} and Tb^{3+}. These advantages suggest that the resultant sensor **1** is a promising fluorescent probe for the detection of heavy metal ions in the environment. Moreover, compound **1** could be used as a probe for the detection of Fe^{3+} ions in cells and bacteria.

Experimental

Materials

2,4-Dimethylpyrrole was purchased from Energy Chemical (Shanghai, China). 4-Hydroxybenzaldehyde, tetrachloro-*p*-benzoquinone and trifluoroacetic acid were purchased from Aladdin Chemical (Shanghai, China). All other reagents were used as received without further purification. Deionized water was used in all experiments.

Preparation of a strong fluorescent Bodipy-containing derivative

The Bodipy derivative was prepared as previously reported with slight modification (32). A mixture of 4-hydroxybenzaldehyde (0.61 g, 5.0 mmol) and 1-bromooctane (1.06 g, 5.5 mmol) in the presence of potassium carbonate (0.83 g, 6.0 mmol) in acetone was heated to reflux for 2 days with stirring under nitrogen. The mixture was cooled to room temperature, and the solvent was removed under reduced pressure. The obtained crude intermediate product was purified by column chromatography on silica gel with petroleum ether/ethyl acetate (20:1 v/v) as the eluent to give the benzaldehyde intermediate product (compound **2**). Yield: 0.82 g, 80%. The prepared benzaldehyde product (0.70 g, 3.4 mmol) and 2,4-dimethylpyrrole (0.65 g, 6.8 mmol) were dissolved in dichloromethane and degassed. After addition of two drops of trifluoroacetic acid to the above solution, the mixture was further stirred for 5 h. The solvent was removed under reduced pressure and purified by column chromatography on silica gel with petroleum ether/ethyl acetate (10:1 v/v) as the eluent to give another intermediate product. The obtained product was dissolved in dichloromethane, tetrachloro-*p*-benzoquinone was added to oxidize the above product and the mixture was stirred for 1 h. Triethylamine (3.1 mL) and boron fluoride ethyl ether (3.2 mL) were then added to the above solution. After stirring for 2 h, the solvent was removed under reduced pressure and the crude product was purified by column chromatography on silica gel with petroleum ether/ethyl acetate (10:1 v/v) as the eluent to give the target molecule (compound **1**). Yield: 568 mg, 37%. ^{1}H NMR (500 Hz, $CDCl_3$, 298 K, relative to Me_4Si)/ppm: δ = 7.15 (d, J = 8.5 Hz, 2H; Bodipy protons at 8-*o*-Ar-position), 6.99 (d, J = 8.5 Hz, 2H; Bodipy protons at 8-*m*-Ar-position), 5.97 (s, 2H; pyrrole protons at 2,6-position), 4.00 (t, J = 6.5 Hz, 2H; -OCH_2-), 2.55 (s, 6H; -CH_3 of Bodipy at 3,5-position), 1.82 (m, 2H; -OCH_2CH_2-), 1.49 (m, 2H; -$OCH_2CH_2CH_2$-), 1.43 (s, 6H; -CH_3 of Bodipy at 1,7-position), 1.33 (m, 8H; -CH_2-), 0.89 (t, J = 7.0 Hz, 3H; -CH_3). ESI-MS: *m/z* 453.2 $[M+H]^+$. Anal. calcd (%) for $C_{27}H_{35}BF_2N_2O$: C, 71.68; H, 7.80; N, 6.19. Found: C, 71.42; H, 7.83; N, 6.31.

Application as a Fe(III) probe

A stock solution of $FeCl_3$ with a concentration of 9 mmol/L was prepared and various Fe^{3+} concentrations were obtained by serial dilution. To check the sensitivity of compound **1**, other ions including Na^+, K^+, Ba^{2+}, Ca^{2+}, Cd^{2+}, Co^{2+}, Cu^{2+}, Fe^{2+}, Hg^{2+}, Mg^{2+}, Mn^{2+}, Zn^{2+}, Pb^{2+}, Cr^{3+}, Er^{3+}, Yb^{3+}, Tb^{3+} and Eu^{3+} were used. All the experiments were similar to the one used for the detection of Fe(III) ions.

Cellular and bacterial imaging

Hep-2 cells were cultured in Dulbecco's modified Eagle's medium supplemented with 10% fetal bovine serum and 1% penicillin/streptomycin (DMEM) using a 96-well plate. Suspensions (30 μg/mL) of compound **1** from the stock solution were prepared with Dulbecco's phosphate buffer saline and DMSO mixed solution (DPBS/DMSO = 1:1 v/v). After sonication for 10 min to ensure complete dispersion, an aliquot (typically 0.01 mL) of the suspension was added to the well of a chamber slide, then incubated at 37°C in a 5% CO_2 incubator for 24 h. Prior to fixation of the Hep-2 cells on the slide for inspection with confocal fluorescence microscopy, the excess compound **1** was removed by washing three times with a warm DPBS and DMSO mixed solution (1:1 v/v).

All *Escherichia coli* bacteria were grown overnight at 37°C in Luria–Bertani medium. After overnight growth, a colony from each bacteria was placed into a 10 mL falcon tube. The bacteria were centrifuged for 5 min at 12000 g, washed twice with sterilized PBS (pH 7.4), and the cell pellet was resuspended in 1 mL of a PBS/DMSO mixed solution (1:1 v/v) of compound **1** (15 μg/mL, pH 7.4) under gentle vortexing. The bacteria with compound **1** were kept at 37°C for 24 h with gentle shaking. After incubation, the mixture was centrifuged to pellet the compound **1**-labeled bacteria, the supernatant was discarded and the pellet was suspended in a PBS/DMSO mixed solution. The process was repeated three times using PBS/DMSO mixed solution (1:1 v/v) to remove all unbound compound **1**. Finally, the pellet was again suspended in 1 mL of a PBS/DMSO mixed solution (1:1 v/v) and fixed on a slide for inspection using confocal fluorescence microscopy.

Characterization methods

^{1}H NMR was recorded on a Bruker DRX 500 (500 MHz) spectrometer (Shanghai, China) with chemical shifts reported relative to tetramethylsilane (Me_4Si). All positive ion ESI-MS were recorded on QTRAP 2000 mass spectrometer (Shanghai, China). Elemental analysis of compound **1** was performed on a Flash EA 1112 elemental analyzer (Shanghai, China). UV–vis absorbance spectra were recorded on a Cary 50 scan spectrophotometer at room temperature. The fluorescence spectra were recorded using a Shimadzu RF-5301 spectrophotometer (Shanghai, China). Cyclic voltammetric measurements were performed by using a CH Instruments Inc. model CHI 660C electrochemical analyzer (Shanghai, China). Electrochemical measurements were performed in dichloromethane solution with 0.1 mol/d^3 ^{n}Bu_4NPF_6 as the supporting electrolyte at room temperature. The reference electrolyte was an $Ag/AgNO_3$ (0.1 mol/d^3 in acetonitrile) electrode

LUMINESCENCE
The Journal of Biological and Chemical Luminescence

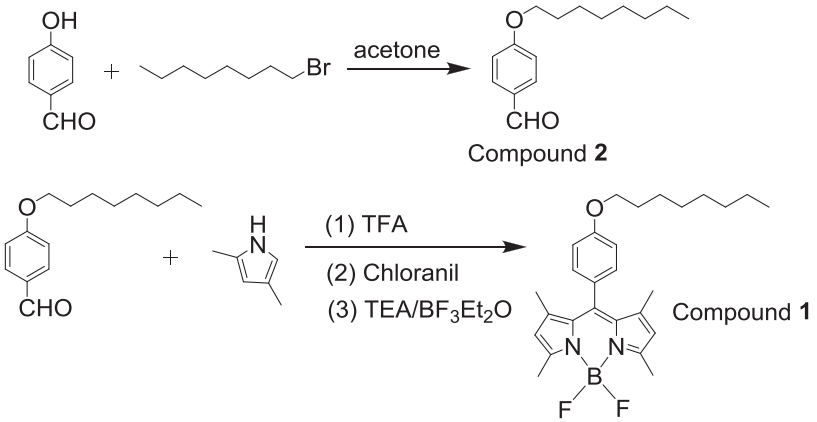

Scheme 1. Synthetic route of compound **1**.

and the working electrode was a glassy carbon electrode (CH Instruments) with a platinum wire as the counter electrode. The working electrode surface was first polished with 1 μm alumina slurry, then rinsed with ultrapure deionized water and sonicated for 5 min in a beaker containing ultrapure water. The polishing and sonication steps were repeated twice and the working electrode was finally rinsed under a stream of ultrapure deionized water. A ferrocenium/ferrocene couple ($FeCp_2^{+/0}$) was used as the internal reference. All solutions for use in the electrochemical studies were deaerated with prepurified argon gas prior to measurement.

General procedure for fluorescence titration

The fluorescence titration of compound **1** with Fe^{3+} was performed as follows: 2 mL of compound **1** (2.5 μmol/L) in a mixed solution of acetonitrile and water (9:1 v/v) was placed in a cuvette, and certain equivalents of Fe^{3+} in water were added to the solution of compound **1** using a micro-injector. Because very small amounts of Fe^{3+} were added, the final volume of the solution was almost unchanged (2 mL). The mixed solution was incubated within 1 min and the corresponding spectra were subsequently measured.

Results and discussion

Synthesis of Bodipy-containing derivative compound 1

The synthetic route for compound **1** used in this study is shown in Scheme 1. Compound **2** was synthesized by the substitution reaction of *p*-hydroxybenzaldehyde with 1-bromooctane in acetone in the presence of potassium carbonate. Compound **1** was prepared by several steps, involving the condensation of compound **2** with 2,4-dimethylpyrrole, oxidation with tetrachloro-*p*-benzoquinone, followed by reaction with boron fluoride ethyl ether. The introduction of an alkyl chain was used to increase the solubility of Bodipy in organic solvent. All the intermediates were characterized using ^{1}H NMR spectroscopy. The final product was characterized by ^{1}H NMR spectroscopy, ESI-MS, and gave satisfactory elemental analysis.

Electrochemical property of compound 1

Compound **1** shows one quasi-reversible oxidation wave at +1.15 V vs. Saturated Calomel Electrode (SCE) in the oxidative scan of its cyclic voltammogram in dichloromethane (0.1 mol/dm^3 ^{n}Bu$_4$NPF$_6$), whereas one quasi-reversible reduction wave at –1.17 V vs. SCE is observed in the reductive scan (Fig. S1). The oxidation and reduction waves are assigned to the oxidation and reduction of Bodipy, respectively, which is consistent with previous studies on Bodipy (33).

Photophysical properties and optical responses of compound 1 to Fe^{3+} ions

The electronic absorption spectrum of compound **1** in a mixed solution of acetonitrile and water (9:1 v/v) shows intense absorption with molar extinction coefficient in the order of 10^4 dm^3/mol/cm at ~ 340–370 nm, which is tentatively assigned to the $S_0 \rightarrow S_2$ transition of Bodipy, consistent with previous reports on the Bodipy system (34). In addition, compound **1** also shows another intense band at 480–510 nm in the electronic absorption spectra. A molar extinction coefficient in the order of 10^4 dm^3/mol/cm, which is assigned to the $S_0 \rightarrow S_1$ transition of Bodipy, is commonly observed in other Bodipy systems (35). Upon addition of Fe^{3+} ions, the absorption spectrum over the range 300–400 nm shows an obvious increase due to the effect of the absorption of Fe^{3+}, but the color of the solution shows no obvious change (Fig. 1).

Upon excitation at λ = 360 nm, compound **1** shows green emission at about 510 nm in a mixture of acetonitrile and water (9:1 v/v) at room temperature, which is assigned to Bodipy-centered emission. The quantum yield of compound **1** reaches 79% using Rhodamine 6G as a standard. It is interesting that the fluorescent

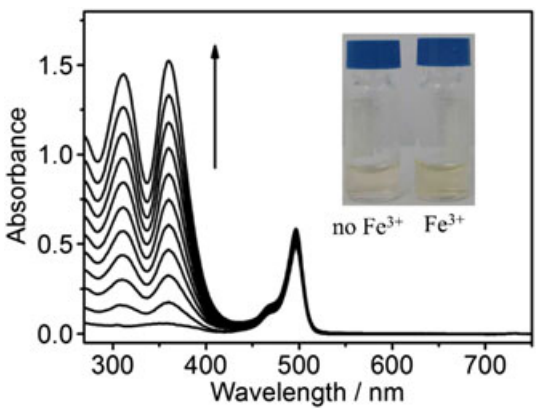

Figure 1. UV–vis absorption spectral changes of compound **1** upon addition of different amounts of Fe^{3+} ion (0, 10, 20, 30, 40, 50, 60, 70, 80, 90 and 100 μmol/L). (Inset) Photograph of compound **1** without and with Fe^{3+} ion (100 μmol/L).

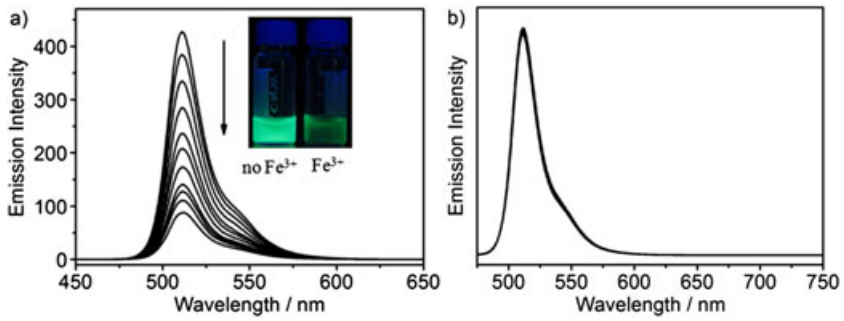

Figure 2. Emission spectral changes of compound **1** upon addition different amounts of Fe^{3+} ion (0, 10, 20, 30, 40, 50, 60, 70, 80, 90 and 100 μmol/L) by excitation at 360 nm (a) and excitation at 460 nm (b). (Inset) Photograph of compound **1** without and with Fe^{3+} ion (100 μmol/L).

intensity gradually decreases with increasing concentrations of Fe^{3+} from 10 to 100 μmol/L (Fig. 2). By contrast, the fluorescent intensity does not show any obvious change on the addition of Fe^{3+} ions upon excitation at λ = 460 nm (Fig. 2). In view of the good spectral overlap between the absorption of Fe^{3+} and the excitation spectrum of compound **1** over the range 300–400 nm (Fig. S2), the mechanism of fluorescent quenching of compound **1** is proposed to be due to absorption of Fe^{3+}. The mechanism is further supported by excitation spectral changes upon addition of different amounts of Fe^{3+} ions measured at an emission of 511 nm (Fig. S3), which shows the lack of fluorescent quenching in the region without the absorption of Fe^{3+}. The emission intensity gradually decreases in the region with the absorption of Fe^{3+} ion with increasing concentrations of Fe^{3+}.

To confirm the proposed mechanism, ^{1}H NMR experiments are performed and ^{1}H NMR spectra of compound **1** before and after the addition of 30 eq. of Fe^{3+} ions are recorded in chloroform (Fig. 3). As expected, there is no obvious change upon addition of Fe^{3+}, which suggests that there is very weak interaction between compound **1** and Fe^{3+}, and fluorescence quenching is the result of the IFE of Fe^{3+}. The results of UV–vis absorbance, photoluminescence and photoluminescence excitation spectra, as well as ^{1}H NMR spectra, confirm that fluorescence quenching arises from the absorbance of Fe^{3+}, ensuring that the IFE occurs in an efficient way.

Response time is a crucial factor in many fluorescent chemosensors. Therefore, the effect of reaction time upon addition of 50 eq. of iron(III) ions was investigated (Fig. 4). Changes in the fluorescence intensity of compound **1** at 512 nm were studied for response times of 0.5–15 min. Figure 4 shows that there is almost no change in the fluorescence intensity at 512 nm within the investigated response time window of 0.5–15 min. Thus, a reaction time of 0.5 min may be used for this system and the data show that compound **1** has a reasonable response time.

For practical purposes, the pH titration of compound **1** was performed to investigate the suitable pH range for iron(III) ion sensing between pH 2.0 and pH 10.0. In the presence of iron(III) ions, the fluorescence intensity is stable over this wide pH range (Fig. 5), which shows the good stability of compound **1** and iron (III) ions within the investigated pH window. Thus, compound **1** could detect iron(III) ions over a wide pH range (2–10).

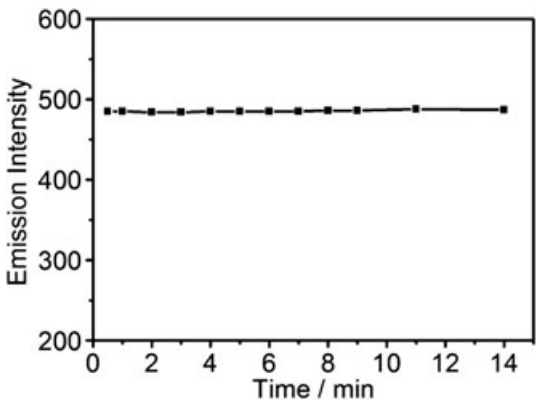

Figure 4. Fluorescence intensity changes on addition of iron(III) (50 eq.) to compound **1** (1×10^{-5} mol/L) in a mixed solution of acetonitrile and water (9:1 v/v) from 1 to 15 min. λ_{em}: 512 nm.

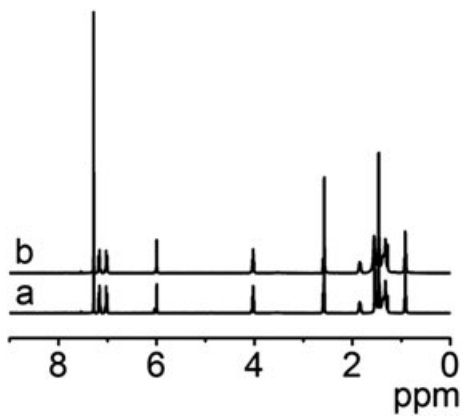

Figure 3. ^{1}H NMR changes in compound **1** in chloroform before (a) and after (b) addition of 30 eq. of Fe^{3+} ion.

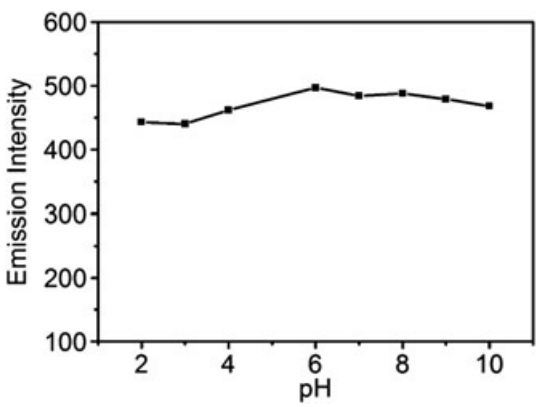

Figure 5. Variation in fluorescence intensity with the pH of compound **1** (1×10^{-5} mol/L) in the presence of iron(III) (50 eq.). λ_{em}: 512 nm.

LUMINESCENCE
The Journal of Biological and Chemical Luminescence

To examine the sensitivity and selectivity of compound **1**, the effect of different types of metal ions (Na^+, K^+, Ba^{2+}, Ca^{2+}, Cd^{2+}, Co^{2+}, Cu^{2+}, Fe^{2+}, Hg^{2+}, Mg^{2+}, Mn^{2+}, Zn^{2+}, Pb^{2+}, Cr^{3+}, Er^{3+}, Yb^{3+}, Tb^{3+} and Eu^{3+}) on the fluorescence was investigated. These ions were studied under the same conditions as Fe^{3+}. Figure 2 shows that the fluorescence intensity of compound **1** was gradually quenched with increasing concentrations of Fe^{3+}. Moreover, a linear proportionality between the logarithm of the fluorescent intensity and the concentration of Fe^{3+} is observed over the range 10–100 μmol/L (Fig. 6). Furthermore, the limit of detection is estimated to be 1.2 μmol/L in terms of a signal-to-noise ratio of 3. By contrast, the fluorescence intensity of compound **1** shows no obvious change upon addition of other metal ions, as shown in Fig. 7. These results indicate that the coexistence of other metal ions does not interfere with the measurement of Fe^{3+}.

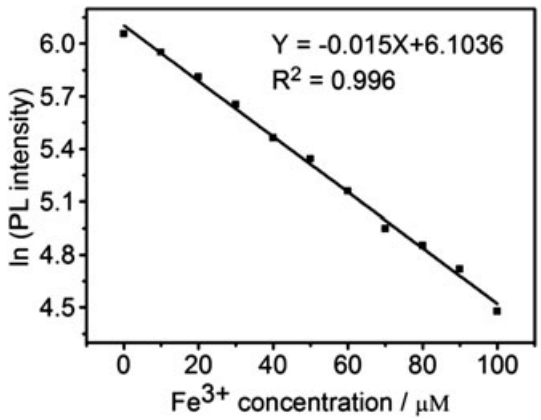

Figure 6. Linear relationship between the logarithm of fluorescent intensity and the concentration of Fe^{3+} ion in a mixed solution of acetonitrile and water (9:1 v/v).

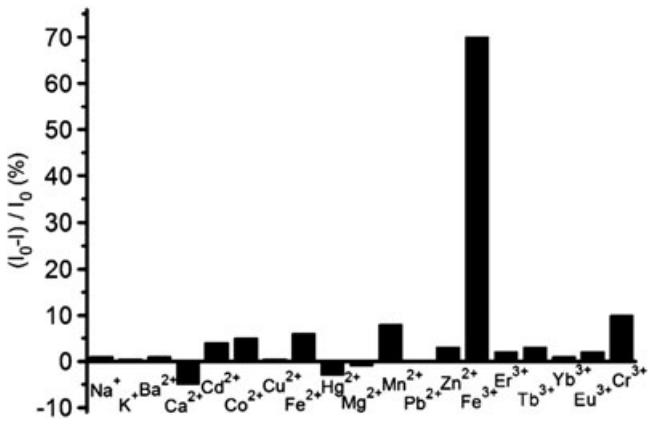

Figure 7. Relative emission intensity (I_0 — I)/I_0 of compound **1** upon addition of 7×10^{-5} mol/L of different metal ions. I_0 and I represent the maximum emission intensity of compound **1** before and after addition of metal ions.

To further assess its application in real water samples, compound **1** was applied to the detection of Fe^{3+} in samples including tap water, mineral water and Tai lake water containing different amounts of Fe^{3+}. Real water samples were first filtered to remove any solid suspension. Studies were performed with 11 concentrations (0, 10, 20, 30, 40, 50, 60, 70, 80, 90 and 100 μmol/L) for each water. It was clear that fluorescent intensity gradually decreases with the increase in the concentration of Fe^{3+}, and a linear relationship between the logarithm of fluorescent intensity of compound **1** and the concentration of Fe^{3+} was observed over the range from 10 to 100 μmol/L (Figs S4–S6). These results indicate that the sensor system is highly sensitive towards Fe^{3+} in real water samples. Furthermore, recovery tests (Table 1) were performed using the three types of water with a fixed amount of Fe^{3+} (10.5, 40.4 and 80.9 μmol/L), and the relative standard deviations (RSD) of the water samples were close to 100% (from 95–105%), which suggests that the fluorescent method performs well for the detection of Fe^{3+} in real water.

Cellular and bacterial applications of compound 1

With a strong red fluorescence, the as-prepared compound **1** showed great potential for use in biological imaging. The cell internalization and intracellular distribution of compound **1** were evaluated using confocal laser fluorescence microscopy. In this study, MTT and an apoptosis assay were used to evaluate the cytotoxicity of compound **1**. As indicated in Fig. 8, the viability of Hep-2 cells remained $>$ 80% after incubation with compound **1**, even after 30 h at a concentration of 60 μg/mL. The results indicate that compound **1** has low acute toxicity. In addition, Fig. 9 reveals the bright field, confocal fluorescence and overlaid imaging of Hep-2 cells incubated with compound **1** for 24 h. As indicated in bright field, Hep-2 cells incubated with compound **1** maintain their normal morphology, suggesting good biocompatibility at this dose and incubation time. Fluorescence images irradiated at 405 nm show green fluorescence within the Hep-2 cells and reveal the uptake behavior of Hep-2 cells. It could also be seen that the fluorescence signal is mostly distributed in the cytoplasm. The results show that compound **1** could be used as a probe for cellular imaging. Interestingly, the fluorescence intensity irradiated with 405 nm is greatly decreased upon addition of Fe^{3+} (10 μM), whereas the fluorescence intensity of compound **1** lacking Fe^{3+} shows a strong green fluorescence (Fig. 10). The results suggest that compound **1** could be used as a probe for measuring Fe^{3+} in cells.

Table 1. Recoveries of iron(III) ion spiked in tap water, mineral water and Tai lake water by compound **1** in a mixed solution of acetonitrile and water (9:1 v/v) using six measuring times of repetition.

	Tap water			Mineral water			Tai lake water		
Added Fe^{3+} (μM)	Found Fe^{3+} (μM)	Recovery (%)	RSD (%)	Found Fe^{3+} (μM)	Recovery (%)	RSD (%)	Found Fe^{3+} (μM)	Recovery (%)	RSD (%)
10.5	10.7	101.9	6.1	11.1	105.7	5.2	11.1	105.7	4.6
40.4	39.8	98.5	5.2	40.1	99.2	3.1	40.9	101.2	3.4
80.9	81.4	100.6	3.5	79.5	98.3	2.2	81.3	100.5	4.3

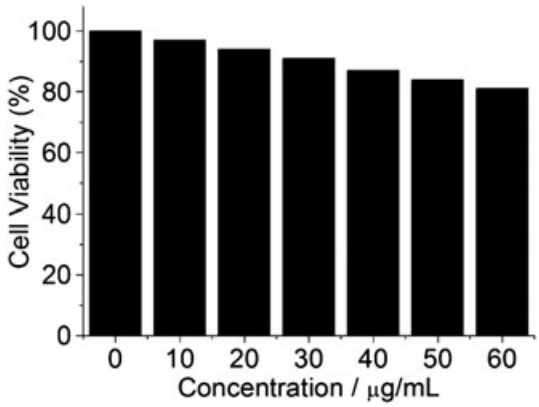

Figure 8. Viability of Hep-2 cells after 24 h incubation with different concentrations of compound **1** in the cell medium, as determined by a MTT assay.

In addition, fluorescence imaging could also be used in *E. coli*. Figure 11 reveals the bright field, confocal fluorescence and overlaid imaging of *E. coli* incubated with compound **1** for 24 h. From the bright field imaging of *E. coli*, we can see that bacteria incubated with compound **1** maintain their normal morphology and exhibit good biocompatibility with compound **1**. As indicated in Fig. 11(b), the bacteria incubated with compound **1** exhibit green fluorescence, suggesting the uptake behavior of *E. coli*. Figure 11(c) demonstrates that the fluorescence signal is distributed over almost the whole bacterium. The results confirm that compound **1** could be used as a probes for bacterial imaging. As expected, upon addition of Fe^{3+}, the fluorescence intensity on irradiation at 405 nm is greatly quenched relative to that free of the Fe^{3+} ion (Fig. 12). The results confirm

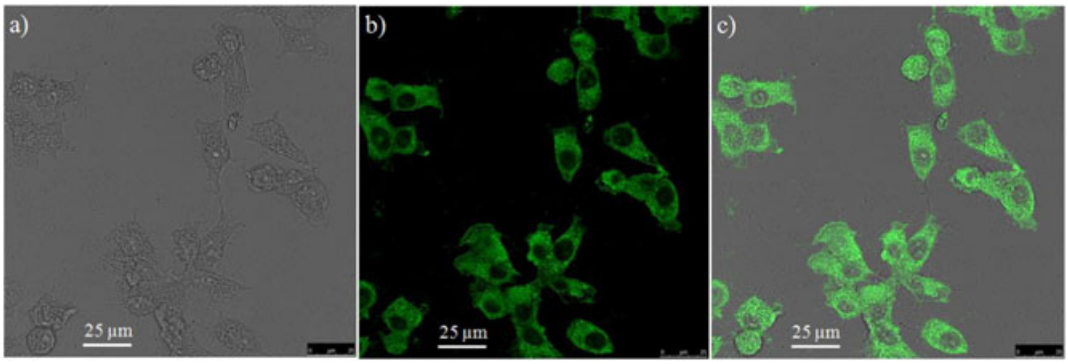

Figure 9. (a) Bright field, (b) confocal fluorescence and (c) overlaid imaging of Hep-2 cell imaging captured by laser scanning confocal microscopy.

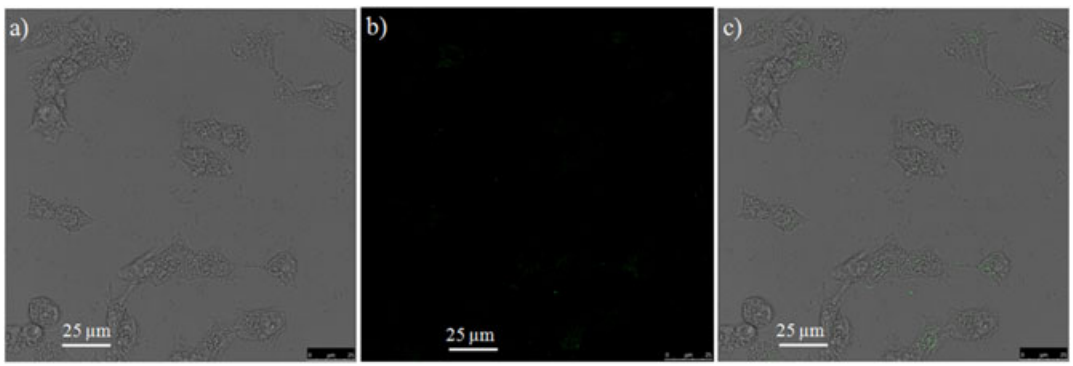

Figure 10. (a) Bright field, (b) confocal fluorescence and (c) overlaid imaging of Hep-2 cell imaging with Fe^{3+} ions (10^{-5} mol/L) captured by laser scanning confocal microscopy.

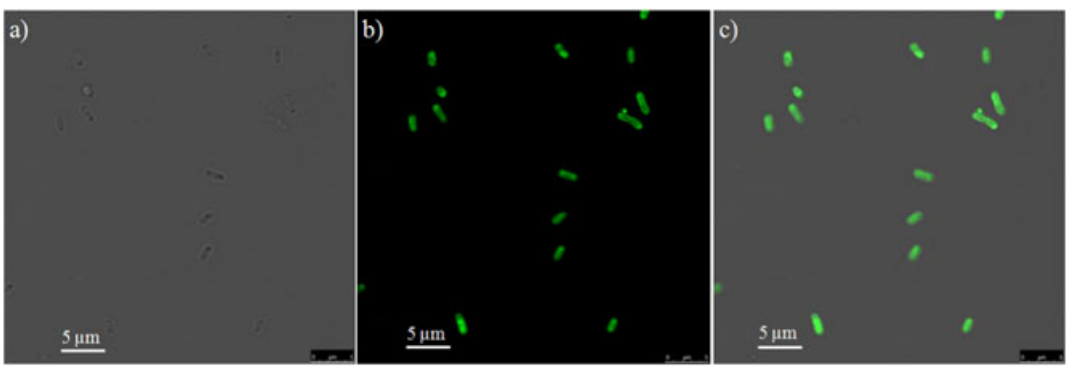

Figure 11. (a) Bright field, (b) confocal fluorescence and (c) overlaid imaging of *E. coli* bacteria imaging captured by laser scanning confocal microscopy.

LUMINESCENCE
The Journal of Biological and Chemical Luminescence

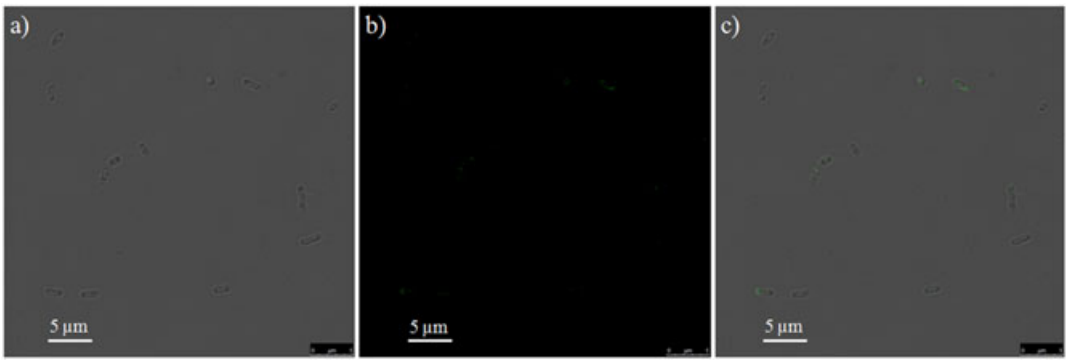

Figure 12. (a) Bright field, (b) confocal fluorescence and (c) overlaid imaging of *E. coli* bacterial imaging with Fe^{3+} ions (10^{-5} mol/L) captured by laser scanning confocal microscopy.

that compound **1** could be used as a probe for monitoring Fe^{3+} in bacteria.

Conclusion

In summary, we have demonstrated a simple, convenient, rapid response, and economical on–off fluorescent method for the detection of Fe^{3+} using Bodipy-containing derivative compound **1** as a fluorescent sensor based on the IFE. The probe appears to have high sensitivity and selectivity relative to conventional methods, with a detection limit of 1.2 μmol/L, and has been demonstrated in real water including tap water, mineral water and Tai lake water. The results suggest that the novel probe has great potential in the detection of Fe^{3+} in environmental samples. In addition, compound **1** could be used as a probe for the detection of iron(III) ions in cells and bacteria. It is anticipated that our method will provide a new perspective on ion detection in environmental and biological samples.

Acknowledgements

This work was supported by the Health Bureau Foundation of Wuxi City, China (MS201524) and Science and Technology Development Foundation Project of Wuxi City, China (CSE31N1429). We also acknowledge support from Wuxi Center for Disease Control and Prevention, China.

References

1. Clarke R, Connolly L, Frizzell C, Elliott CT. Challenging conventional risk assessment with respect to human exposure to multiple food contaminants in food: a case study using maize. Toxicol Lett 2015;238:54–64.
2. Xiao Q, Zong Y, Lu S. Assessment of heavy metal pollution and human health risk in urban soils of steel industrial city (Anshan), Liaoning, Northeast China. Ecotox Environ 2015;120:377–85.
3. Kaplan ME, Simmons ER, Hawkins JC, Ruane LG, Carney JM. Quantitative analysis of the fatty acid content in flax seeds (*Linum usitatissimum*) as influenced by soil cadmium and mycorrhizal fungi. J Sci Food Agr 2014;95:2528–32.
4. Beinert H, Kennedy MC, Stout CD. Aconitase as iron−sulfur protein, enzyme, and iron-regulatory protein. Chem Rev 1996;96:2335–74.
5. Zhu J, Dizin E, Hu X, Wavreille AS, Park J, Pei D. S-Ribosylhomocysteinase (LuxS) is a mononuclear iron protein. Biochemistry 2003;42:4717–26.
6. Burdo JR, Connor JR. Brain iron uptake and homeostatic mechanisms: an overview. BioMetals 2003;16:63–75.
7. Yamamoto K, Kawanishi S. Site-specific DNA damage by phenylhydrazine and phenelzine in the presence of copper(II) ion or iron(III) complexes: roles of active oxygen species and carbon radicals. Chem Res Toxicol 1992;5:440–6.
8. Lesniak W, Pecoraro VL, Schacht J. Ternary complexes of gentamicin with iron and lipid catalyze formation of reactive oxygen species. Chem Res Toxicol 2005;18:357–64.
9. Hilger J, Goerig T, Weber P, Hoeft B, Eggersdorfer M, Carvalho NC, et al. Micronutrient intake in healthy toddlers: a multinational perspective. Nutrients 2015;7:6938–55.
10. He YH, Lai JP, Sun H, Chen ZM, Lan S. A fast, sensitive and stable fluorescent fiber-optic chemosensor for quantitative detection of Fe^{3+} in real water and HepG2 living cells. Sensor Actuat B-Chem 2016;225:405–12.
11. Wei R, Wei Z, Sun L, Zhang JZ, Liu J, Ge X, et al. Nile Red derivative-modified nanostructure for upconversion luminescence sensing and intracellular detection of Fe^{3+} and MR imaging. ACS Appl Mater Interface 2016;8:400–10.
12. Faizi MSH, Gupta S, Jain VK, Sen P. Highly selective visual detection of Fe^{3+} at ppm level. Sensor Actuat B-Chem 2016;222:15–20.
13. Willis RC. A new perspective on subnanomolar iron detection. Anal Chem 2008;80:4786.
14. Sui B, Tang S, Liu T, Kim B, Belfield KD. Novel BODIPY-based fluorescence turn-on sensor for Fe^{3+} and its bioimaging application in living cells. ACS Appl Mater Interface 2014;6:18408–12.
15. Bricks JL, Kovalchuk A, Trieflinger C, Nofz M, Büschel M, Tolmachev AI, et al. On the development of sensor molecules that display Fe(III)-amplified fluorescence. J Am Chem Soc 2005;127:13522–9.
16. Kagit R, Yildirim M, Ozay O, Yesilot S, Ozay H. Phosphazene based multicentered naked-eye fluorescent sensor with high selectivity for Fe^{3+} ions. Inorg Chem 2014;53:2144–51.
17. Kong L, Wong HL, Tam AYY, Lam WH, Wu L, Yam VWW. Synthesis, characterization, and photophysical properties of Bodipy–spirooxazine and –spiropyran conjugates: modulation of fluorescence resonance energy transfer behavior via acidochromic and photochromic switching. ACS Appl Mater Interface 2014;6:1550–62.
18. Basa PN, Bhowmick A, Schulz MM, Sykes AG. Site-selective imination of an anthracenone sensor: selective fluorescence detection of barium(II). J Org Chem 2011;76:7866–71.
19. Dodani SC, Leary SC, Cobine PA, Winge DR, Chang CJ. A targetable fluorescent sensor reveals that copper-deficient SCO1 and SCO2 patient cells prioritize mitochondrial copper homeostasis. J Am Chem Soc 2011;133:8606–16.
20. Zheng M, Xie Z, Qu D, Li D, Du P, Jing X, et al. On off on fluorescent carbon dot nanosensor for recognition of chromium(VI) and ascorbic acid based on the inner filter effect. ACS Appl Mater Interface 2013;5:13242–7.
21. Kim H, Lee B, Byeon SH. The inner filter effect of Cr(VI) on Tb-doped layered rare earth hydroxychlorides: new fluorescent adsorbents for the simple detection of Cr(VI). Chem Commun 2015;51:725–8.
22. Street KW, Tarver M. Fluorescence inner filtering in double-pass cell configurations. Part 4. Interdependence of primary and secondary inner filtering. Analyst 1988;113:347–9.
23. Street KW. Fluorescence inner filtering in double-pass cell configurations. Part 1. Primary inner filtering. Analyst 1985;110:1169–72.
24. Bessette A, Hanan GS. ChemInform Abstract: Design, synthesis and photophysical studies of dipyrromethene-based materials: insights

into their applications in organic photovoltaic devices. Chem Soc Rev 2014;43:3342–405.
25. Boens N, Leen V, Dehaen W. Fluorescent indicators based on BODIPY. Chem Soc Rev 2012;41:1130–72.
26. Ziessel R, Harriman A. Artificial light-harvesting antennae: electronic energy transfer by way of molecular funnels. Chem Commun 2011;47:611–31.
27. Zhu H, Fan J, Wang B, Peng X. Fluorescent, MRI, and colorimetric chemical sensors for the first-row d-block metal ions. Chem Soc Rev 2015;44:4337–66.
28. Sahoo SK, Sharma D, Bera RK, Crisponi G, Callan JF. Iron(III) selective molecular and supramolecular fluorescent probes. Chem Soc Rev. 2012;41:7195–227.
29. Kursunlu AN, Guler E, Ucan HI, Boyle RW. A novel Bodipy–dipyrrin fluorescent probe: synthesis and recognition behaviour towards Fe(II) and Zn(II). Dye Pigment 2012;94:496–502.
30. Kursunlu AN, Sahin E, Güler E. Bodipy/dipyridylamino-based 'turn-on' fluorescent chemosensor for trivalent chromium cations: characterization and photophysical properties. RSC Adv 2015;5:5951–7.
31. Kursunlu AN. A fluorescent 'turn on' chemosensor based on Bodipy–anthraquinone for Al(III) ions: synthesis and complexation/spectroscopic studies. RSC Adv 2015;5:41025–32.
32. Yuan M, Zhou W, Liu X, Zhu M, Li J, Yin X, et al. A multianalyte chemosensor on a single molecule: promising structure for an integrated logic gate. J Org Chem 2008;73:5008–14.
33. Nepomnyashchii AB, Bard AJ. Electrochemistry and electrogenerated chemiluminescence of BODIPY dyes. Acc Chem Res 2012;45:1844–53.
34. Ulrich G, Ziessel R, Harriman A. Die vielseitige Chemie von Bodipy-Fluoreszenzfarbstoffen. Angew Chem 2008;120:1202–19.
35. Lu JS, Ko SB, Walters NR, Wang S. Decorating BODIPY with three- and four-coordinate boron groups. Org Lett 2012;14:5660–3.

Supporting Information

Additional supporting information may be found in the online version of this article at the publisher's web site.